

Comparison of different modulations of photoplethysmography in extracting respiratory rate: from a physiological perspective

Liu, H, Chen, F, Hartmann, V, Khalid, SG, Hughes, S & Zheng, D

Published PDF deposited in Coventry University's Repository

Original citation:

Liu, H, Chen, F, Hartmann, V, Khalid, SG, Hughes, S & Zheng, D 2020, 'Comparison of different modulations of photoplethysmography in extracting respiratory rate: from a physiological perspective', *Physiological Measurement*, vol. 41, no. 9, 094001.

<https://dx.doi.org/10.1088/1361-6579/abaaf0>

DOI 10.1088/1361-6579/abaaf0

ISSN 0967-3334

ESSN 1361-6579

Publisher: IOP

Original content from this work may be used under the terms of the Creative Commons Attribution 3.0 license. Any further distribution of this work must maintain attribution to the author(s) and the title of the work, journal citation and DOI.

Copyright © and Moral Rights are retained by the author(s) and/ or other copyright owners. A copy can be downloaded for personal non-commercial research or study, without prior permission or charge. This item cannot be reproduced or quoted extensively from without first obtaining permission in writing from the copyright holder(s). The content must not be changed in any way or sold commercially in any format or medium without the formal permission of the copyright holders.



PAPER

OPEN ACCESS

RECEIVED

19 February 2020

REVISED

28 July 2020

ACCEPTED FOR PUBLICATION

30 July 2020

PUBLISHED



1 October 2020

Original content from this work may be used under the terms of the [Creative Commons Attribution 3.0 licence](#).

Any further distribution of this work must maintain attribution to the author(s) and the title of the work, journal citation and DOI.



Comparison of different modulations of photoplethysmography in extracting respiratory rate: from a physiological perspective

Haipeng Liu¹ , Fei Chen² , Vera Hartmann³, Syed Ghufan Khalid¹, Stephen Hughes³ and Dingchang Zheng¹

¹ Research Centre for Intelligent Healthcare, Faculty of Health and Life Sciences, Coventry University, Coventry, CV1 5FB, United Kingdom

² Department of Electrical and Electronic Engineering, Southern University of Science and Technology, Shenzhen, 518055, People's Republic of China

³ School of Allied Health, Faculty of Health, Education, Medicine, and Social Care, Anglia Ruskin University, Chelmsford, CM1 1SQ, United Kingdom

E-mail: dingchang.zheng@coventry.ac.uk and fchen@sustech.edu.cn

Keywords: photoplethysmography (PPG), respiratory frequency, respiratory modulation

Abstract

Objective: Based on different physiological mechanisms, the respiratory modulations of photoplethysmography (PPG) signals differ in strength and resultant accuracy of respiratory frequency (RF) estimations. We aimed to investigate the strength of different respiratory modulations and the accuracy of resultant RF estimations in different body sites and two breathing patterns. **Approach:** PPG and reference respiratory signals were simultaneously measured over 60 s from 36 healthy subjects in six sites (arm, earlobe, finger, forehead, wrist-under (volar side), wrist-upper (dorsal side)). Respiratory signals were extracted from PPG recordings using four demodulation approaches: amplitude modulation (AM), baseline wandering (BW), frequency modulation (FM) and filtering. RFs were calculated from the PPG-derived and reference respiratory signals. To investigate the strength of respiratory modulations, the energy proportion in the range that covers 75% of the total energy in the reference respiratory signal, with RF in the middle, was calculated and compared between different modulations. Analysis of variance and the Scheirer–Ray–Hare test were performed with *post hoc* analysis. **Main results:** In normal breathing, FM was the only modulation whose RF was not significantly different from the reference RF ($p > 0.05$). Compared with other modulations, FM was significantly higher in energy proportion ($p < 0.05$) and lower in RF estimation error ($p < 0.05$). As to energy proportion, measurements from the finger and the forehead were not significantly different ($p > 0.05$), but both were significantly different from the other four sites ($p < 0.05$). In deep breathing, the RFs derived by BW, filtering and FM were not significantly different from the reference RF ($p > 0.05$). The RF estimation error of FM was significantly less than that of AM or BW ($p < 0.05$). The energy proportion of FM was significantly higher than that of other modulations ($p < 0.05$). **Significance:** Of all the respiratory modulations, FM has the highest strength and is appropriate for accurate RF estimation from PPG signals recorded at different sites and for different breathing patterns.

1. Introduction

Respiratory frequency (RF) is an important physiological parameter in healthcare monitoring, especially for patients with respiratory diseases. Respiratory rate (RR) is a vital sign that is directly derived from RF. However, long-term monitoring of RF is difficult due to the various limitations of current respiratory monitoring devices, which are expensive, difficult to use and could cause discomfort to patients. Some new devices, such as inertial sensors, provide the possibility of convenient monitoring of RF, but still need further validation for clinical use or long-term monitoring. It has been suggested that long-term RF monitoring can be achieved by extracting RF from other signals recorded by wearable sensors (Liu *et al* 2019).

In particular, RF may be easily extracted from photoplethysmography (PPG) signals. A PPG signal reflects the blood volumetric changes in the peripheral microvascular bed and is continuously recorded by wearable sensors. Therefore, PPG finds wide application in healthcare. During respiration, the PPG signal is modulated by several physiological factors in its amplitude, baseline, and frequency (Charlton *et al* 2017a). These factors reflect the influence of respiratory movement on the hemodynamics of peripheral arterioles and capillaries. The respiratory modulation of PPG signals is related to the complex interaction of different physiological mechanisms such as vasoconstriction, interthoracic pressure change, and vagal outflow (Meredith *et al* 2012). Meanwhile, other influences on the modulation of the PPG signal exist, including baroreceptor reflex and neural tone (Kiselev *et al* 2016).

To derive RF, the majority of current algorithms demodulate the respiratory signal from a PPG signal based on amplitude modulation (AM), baseline wandering (BW), and frequency modulation (FM) (Charlton *et al* 2017a). Here the amplitude refers to the magnitude of fluctuation or the difference between the maximum and minimum values of PPG signal in a cardiac cycle. The baseline refers to the minimum value of the PPG signal in a cardiac cycle. To enhance the reliability and robustness of these algorithms, some studies have investigated the fusion of RF values derived by AM, BW and FM (Liu *et al* 2019). However, the accuracy of PPG-derived RF estimation using fusion techniques varies in different studies (Orphanidou 2017, Birrenkott *et al* 2018). In a widely used Smart Fusion algorithm, the error is 2.8 ± 3.4 breaths min^{-1} , or 0.047 ± 0.057 Hz, which is beyond the clinically reliable range (<2 breaths min^{-1}) (Karlen *et al* 2013). To improve the accuracy of PPG-based RF estimation, it is necessary to comprehensively investigate the differences between different respiratory modulations in strength that directly influence the accuracy of RF estimation. Moreover, while current fusion algorithms focus on signal processing as well as the statistical and probabilistic characteristics of signals, there is a lack of analysis of the physiological mechanisms that underlie the different respiratory modulations.

This study aims to provide a preliminary comparison of different respiratory modulations of PPG signal in their strength and accuracy of resultant RF estimation from a physiological perspective. RF is estimated by different modulation algorithms from PPG signals of different body sites under different breathing patterns. The intensities of different respiratory modulations are also compared. Finally, we analyse the physiological effect of the measurement site and breathing pattern on the strength of respiratory modulation and the accuracy of RF estimation.

2. Methods

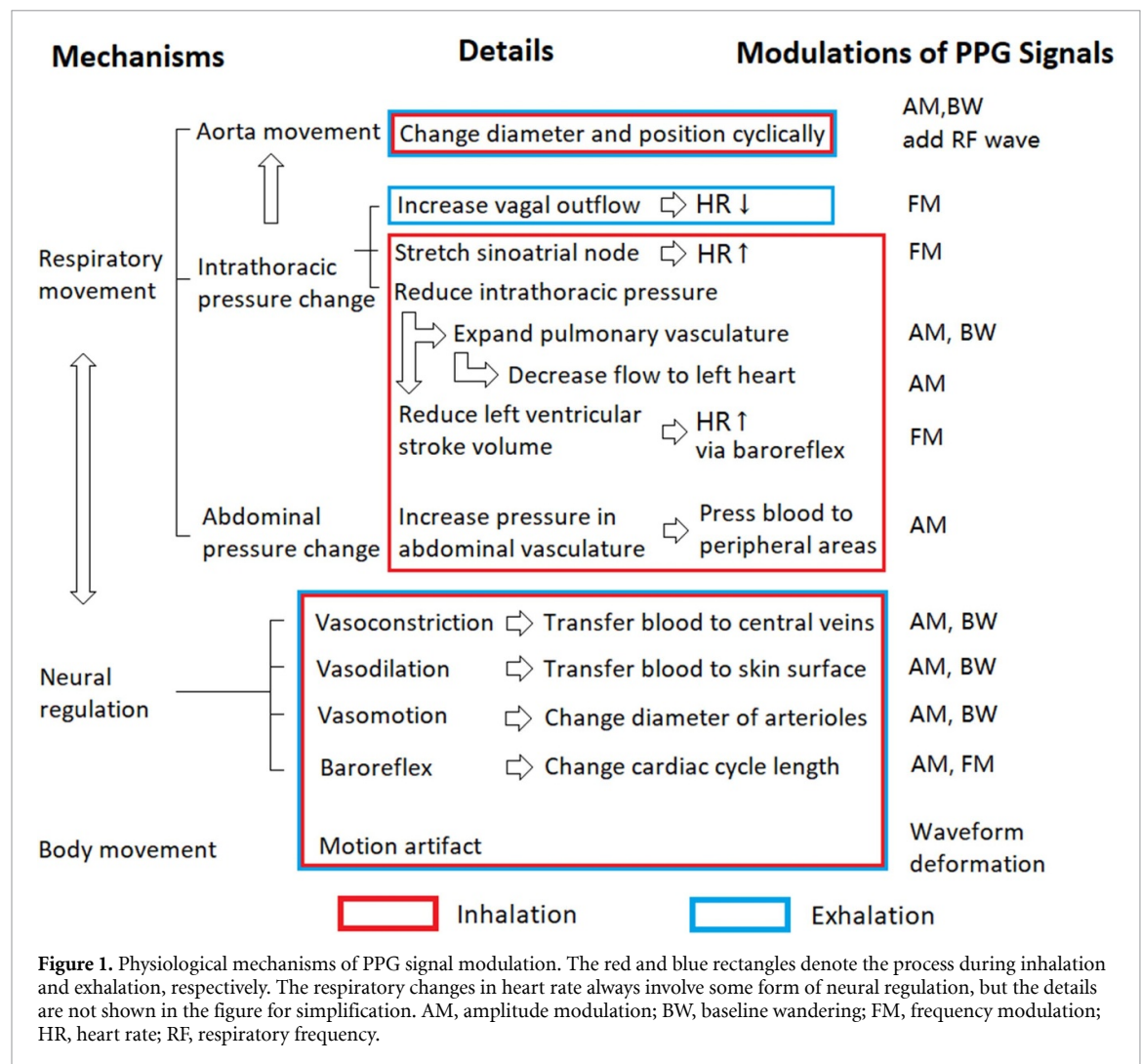
2.1. Analysis of respiratory modulations of PPG signal from a physiological perspective

A PPG signal is an optical signal collected from volumetric changes in the peripheral microcirculation. The blood ejected from the left ventricle flows through aorta and major arteries into arterioles and capillaries where PPG signal is recorded. The photocurrent of the sensor is then transformed to voltage in the recorded PPG signals. The blood then flows through the venous system back to the left heart via the pulmonary circulation. Factors influencing the PPG waveform include those related to sensor attachment, such as any movement and the pressure exerted between the PPG sensor and the skin. These factors can nonlinearly change the waveform, leading to noises in the recorded PPG signal.

It is widely known that neural regulation can influence respiratory movement. It has been disclosed that respiratory movement causes variation in sympathetic tone control of cutaneous blood vessels (as detailed below). The interaction between neural regulation and respiratory movement has a complicated effect on the respiratory modulations of PPG signals (Nilsson *et al* 2000, Johansson 2003).

Charlton *et al* have extensively reviewed the mechanisms of AM, BW and FW (Charlton *et al* 2017b) (Charlton *et al* 2017a). Recently, some new mechanisms of respiratory modulation have been proposed such as vasomotor (Ovadia-Blechman *et al* 2017) and aortic movement (Sailer *et al* 2015). Here we categorize the mechanisms of respiratory modulations on PPG signals from a physiological perspective.

During respiration, the PPG signal is modulated by respiratory movements as well as related neural regulations, and is influenced by motion artefacts, as shown in figure 1. It has been demonstrated that the aorta and its branches undergo considerable respiratory movement (Sailer *et al* 2015), which could change the blood flow, as well as the resistance and capacity of the arteries. Resultantly, AM and BW will appear in PPG waveform, with an additional pulsative wave whose frequency is RF superimposed to the PPG wave. Thoracic movement is a major cause of respiratory modulations. Firstly, the thoracic pressure changes contribute to the movement of the aorta. Secondly, the intrathoracic pressure change stretches sinoatrial node during inhalation and increases the vagal outflow during exhalation, with the heart rate (HR) increased and decreased, causing respiratory sinus arrhythmia (RSA). RSA is the major mechanism of FM in PPG signal. During inhalation, the pulmonary vasculature is expanded due to reduced intrathoracic pressure, which in turn decreases the resistance and increases the capacity of veins and right heart. Consequently, the



blood flow to left ventricular is reduced, with the stroke volume decreased. Thus, the magnitude of PPG signal will be decreased, which leads to AM and BW in the PPG signal. Due to the decreased blood pressure detected by baroreceptors, HR is then increased via baroreflex regulation, resulting in FM in PPG signal. During inhalation, increased pressure in abdominal vasculature could impulse the blood to peripheral areas, causing AM and BW in the PPG waveform. The exact change of blood flow depends on the balance or opposite effects exerted by thoracic and abdominal movements (Khoo and Chalacheva 2019). The neural regulations include vasoconstriction, vasomotion, and baroreflex. Vasoconstriction happens during inhalation when blood is transferred to veins, resulting in BW in PPG signal. In subjects whose body temperatures have been sufficiently lowered, the deep inspiration protocol can result in vasodilation rather than vasoconstriction (Khoo and Chalacheva 2019). Vasomotion directly changes the diameter of arterioles, especially during slow breathing at low oxygenation levels (Ovadia-Blechman *et al* 2017). The change of microcirculatory resistance results in AM and BW in PPG signals. The baroreflex changes the stroke volume and HR according to blood pressure, forming a closed-loop control system, which directly incurs AM and FM in PPG waveform. The periodic respiratory movement and blood flow changes commonly contribute to the additional wave superimposed on the PPG signals, which can be extracted with filtering for RF estimation. Additionally, the motion artefact causes a change of attachment and pressure, which further deforms the PPG waveform.

2.2. Collection of PPG and reference respiratory signals

Thirty-six healthy adult subjects (12 males and 24 females, mean \pm SD and range of age: 33 ± 12 yrs, 19–58 years) participated in the experiment. For each subject, PPG signals were measured in sitting posture from six different body sites in a random sequence: arm, earlobe, finger, forehead, as well as volar and dorsal sides of the wrist (denoted as wrist-under and wrist-upper, respectively). Simultaneously, the reference respiratory signal was measured by a strain gauge on a thoracic belt. Each measurement lasted for one

minute. The sampling rate was 2000 Hz for all signals. The PPG signals were collected from the PPG100C module of the BIOPAC System (BIOPAC Systems, Inc. Goleta, CA), which has preset hardware filters including a low-pass filter (cut-off frequency: 10 Hz) and a high pass filter (cut-off frequency: 0.05 Hz) to remove the direct current component. The recorded waveform of PPG signal was clear. The respiratory module also contains preset hardware filters including a low pass filter (cut-off frequency: 1 Hz) and a high-pass filter (cut-off frequency: 0.05 Hz), with which a clear waveform of respiratory signals can be recorded. Therefore, no software filter was applied during data collection. The data collection details have been described in our previous work (Hartmann *et al* 2019).

2.3. RF extraction by demodulation

From the analysis above, the PPG signal is modulated by four different respiratory modulations: AM, BW, FM and the additional wave with RF as its frequency. Therefore, RF could be estimated from the respiratory signals extracted from the PPG signal using demodulation techniques based on AM, BW, FM and direct filtering.

2.3.1. Pre-processing of PPG signal

The recorded data were imported to MATLAB (R2018a; The MathWorks Inc. Natick, USA). To reduce the high-frequency noises which may affect the selection of peak (systolic maximum) and valley (end-of-diastolic trough) points, the original PPG signal was pre-processed with the low-pass infinite impulse response (IIR) filter whose pass band and stop bands are <3 Hz and >5 Hz, respectively.

2.3.2. Extraction of respiratory signals

AM and BW: In the filtered PPG signal, the valley and peak points were selected, as shown in figure 2(a). Firstly, the difference function of the PPG signal was calculated: $\text{diff}(i) = \text{PPG}(i) - \text{PPG}(i-1)$, where i

denotes the sequence of sampling. Secondly, all the points which satisfy
$$\begin{cases} \text{diff}(i+1) \cdot \text{diff}(i) \leq 0 \\ \text{diff}(i) > 0 \\ \text{diff}(i+1) \leq 0 \end{cases} \quad \text{and}$$

$$\begin{cases} \text{diff}(i+1) \cdot \text{diff}(i) \leq 0 \\ \text{diff}(i) < 0 \\ \text{diff}(i+1) \geq 0 \end{cases}$$
 were selected as the candidate points for peaks and valleys, respectively. Next, a

candidate point of peak was excluded if there was another point within ± 0.1 s range with a higher value of PPG signal. Similarly, a candidate point of valley was excluded if there was another point within ± 0.1 s range with a lower value of PPG signal. The diastolic notch and local extreme points were therefore excluded. Finally, between two consecutive peaks, only one valley with the lowest value of PPG signal was selected, and vice versa. Two curves derived by cubic spline interpolation were used to connect the peaks and valleys, respectively. The curve which connects valleys reflected the fluctuation of baseline, therefore was used as the respiratory signal derived by BW. By subtracting the peak and valley curves, the derived curve reflects the fluctuations of amplitude; therefore this was used as the respiratory signal derived by AM.

FM: The filtered PPG signal was further processed to extract respiratory signal by FM. The continuous PPG signal was divided by the valley points into different cardiac cycles. In each cycle, the start and end points (two consecutive valley points) were connected by a segment whose function is linear. The waveform was finally detrended by subtracting the linear function in each cycle (figure 2(b)). The BW effect was excluded. In each cycle, the point of the maximal slope was selected by calculating the derivative of the detrended PPG signal. The maximal slope point is located at the systolic uprising side of the PPG signal. The time intervals between consecutive maximal slope points were calculated. The FM-based respiratory signal was derived from the variability of intervals based on pulse interval modulation (PIM) (Hartmann *et al* 2019) (figure 2(c)).

Filtering: The filtered PPG signal before extraction of peaks and valleys was downsampled in 500 Hz, then filtered with another low-pass IIR filter whose pass and stop bands were <0.6 Hz and >1.0 Hz. The resultant signal was the respiratory signal derived directly by filtering (figure 2(d)).

2.3.3. Estimation of RF

The four respiratory signals extracted from PPG by AM, BW, FW and filtering, as well the reference respiratory signal recorded by the respiratory belt (figure 2(e)), were processed with discrete Fourier transformation (DFT). The focus of this study is the comparison between different respiratory modulations instead of the improvement of RF estimation accuracy. Therefore, the original respiratory signals were used. The periodogram function in the Signal Processing Toolbox of MATLAB was used to get the power spectral density (PSD). The respiratory signals had been downsampled before calculating PSD. The downsampling rate was 8 Hz. In PSD, a rectangular window with the same length as the input signal was used, with the

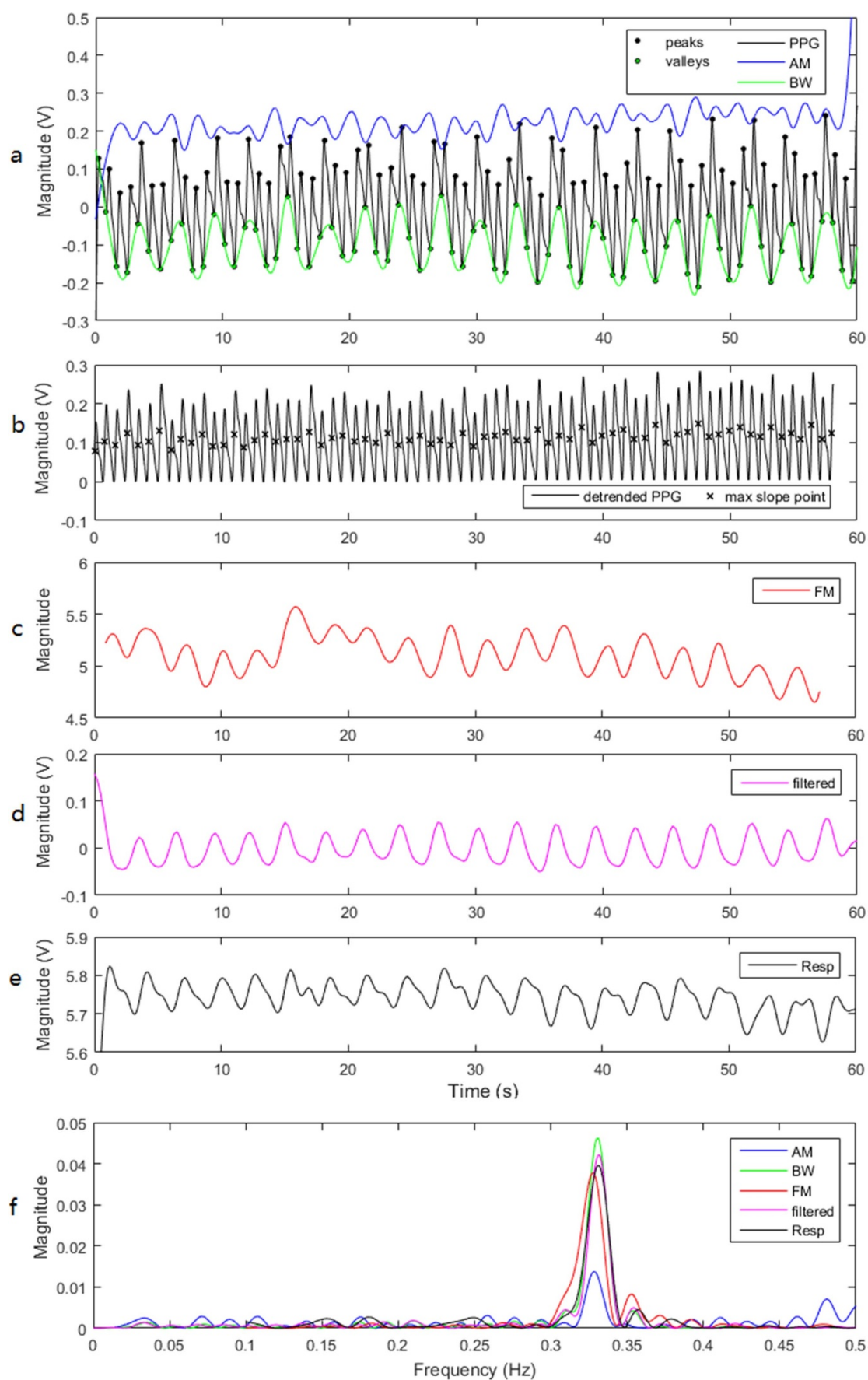


Figure 2. Estimation of respiratory rate from PPG signals using different modulations. (a) Extraction of peaks and valleys from the filtered PPG signal recorded in normal breathing. The blue and green lines denote the derived respiratory signals by AM and BW. (b) Extraction of maximal slope points (marked by crosses) from detrended PPG signal. (c) Respiratory signal derived by FM. (d) Respiratory signal derived by filtering. (e) Reference respiratory signal (Resp) recorded by strain gauge. (f) Extraction of RF from different respiratory signals using power spectral density.

frequency range of 0.05 Hz to 0.3 Hz for deep breathing and 0.1 Hz to 0.5 Hz for normal breathing. The RF resolution was 0.001 Hz, which was equal to 0.06 breath per minute in RR. The peak frequency was selected as the estimated RF (figure 2(f)).

2.3.4. Calculation of energy proportion

To quantitatively estimate the strength of each respiratory modulation, the energy ratio was calculated. In the PSD of the reference respiratory signal, the peak which indicates RF has the highest density of energy. A range of frequency (denoted as ‘75%-respiratory interval’) was calculated, which covers 75% of total energy (total area under the PSD curve) with RF in the middle. On the corresponding PSD of each PPG-derived respiratory signal, the proportion of energy in the ‘75%-respiratory interval’ was calculated. This value reflects the ratio of respiratory-related energy in the respiratory signal, thus indicating the strength of corresponding respiratory modulation.

2.4. Statistical analysis

Statistical analysis was performed using SPSS (Version 24.0, IBM Corp) and R programming language (R Core Team (2019). R: A language and environment for statistical computing. R Foundation for Statistical Computing). Since RF was paced at a fixed rate of 0.1 Hz in deep breathing, the data of normal and deep breathing patterns were analysed separately.

The relative error of each PPG-derived RF value was calculated: $ERF = \frac{RF_{PPG} - RF_{resp}}{RF_{resp}}$, where RF_{PPG} , RF_{resp} and ERF denote the PPG-derived RF, the corresponding RF derived from the respiratory belt and the estimation error of PPG-derived RF. The RF and ERF values derived by different methods (AM, BW, FM, filtering) from different measurement sites (arm, earlobe, finger, forehead, wrist-under, wrist-upper) were compared to investigate if there is any significant influence of RF extraction method, measurement site, or their interaction, on RF or ERF values. Firstly, Levene’s test was performed to investigate the homogeneity of variance (defined as $p > 0.05$). If the hypothesis of homogeneity of variance was satisfied, the analysis of variance (ANOVA) was performed. If the assumption was violated ($p < 0.05$), the Scheirer–Ray–Hare test was performed as a substitute. If any significant influence was observed, in ANOVA, least significant difference (LSD) *post hoc* multiple comparisons were performed to find the pairs with significant difference ($p < 0.05$). In the Scheirer–Ray–Hare test, Dunn’s Kruskal–Wallis multiple comparisons were performed for *post hoc* analysis. The p-value was adjusted with the Benjamini–Hochberg method.

To illustrate the difference between different RF extraction methods and different measurement sites in the accuracy of RF estimation, Bland–Altman analysis was performed on PPG-derived and reference RFs.

3. Results

3.1. Energy proportion

The results showed that the energy ratio was significantly influenced by measurement site, extraction method, and their interaction ($p < 0.05$ for all, homogeneity of variance satisfied). The strongest modulation was FM at the finger, and FM was often stronger than the other modulations, particularly during deep breathing, as shown in figure 3.

Normal breathing: For normal breathing, the homogeneity of variance was satisfied by the overall distribution of energy proportion ($p = 0.056$ in Levene’s test). Therefore, ANOVA was performed. The results showed that the energy ratio was significantly influenced by measurement site, extraction method, and their interaction ($p < 0.05$ for all).

The results of *post hoc* analysis showed that the energy ratio derived by FM was significantly different from the results derived by other methods (AM, BW, filtering) ($p < 0.05$ for all). There was no significant difference among the results derived by AM, BW and filtering ($p > 0.05$ for all).

As to the comparison between sites, finger and forehead were not significantly different ($p > 0.05$), but both were significantly different from the results from the other four sites (arm, earlobe, wrist-under, wrist-upper) ($p < 0.05$ for all). There was no significant difference among the results from these four sites ($p > 0.05$ for all).

Deep breathing: For deep breathing, the homogeneity of variance was violated by the overall distribution of energy proportion ($p < 0.05$ in Levene’s test). Therefore, the Scheirer–Ray–Hare test was performed. The results showed that the energy ratio was significantly influenced by extraction method ($p < 0.01$), without any significant influence from the site, or the interaction between site and extraction method ($p > 0.05$ for all).

The *post hoc* analysis showed that the energy ratios derived by different methods were always significantly different ($p < 0.05$ for all) except between BW and filtering ($p > 0.05$). There was no significant difference between the results of any two different sites ($p > 0.05$ for all).

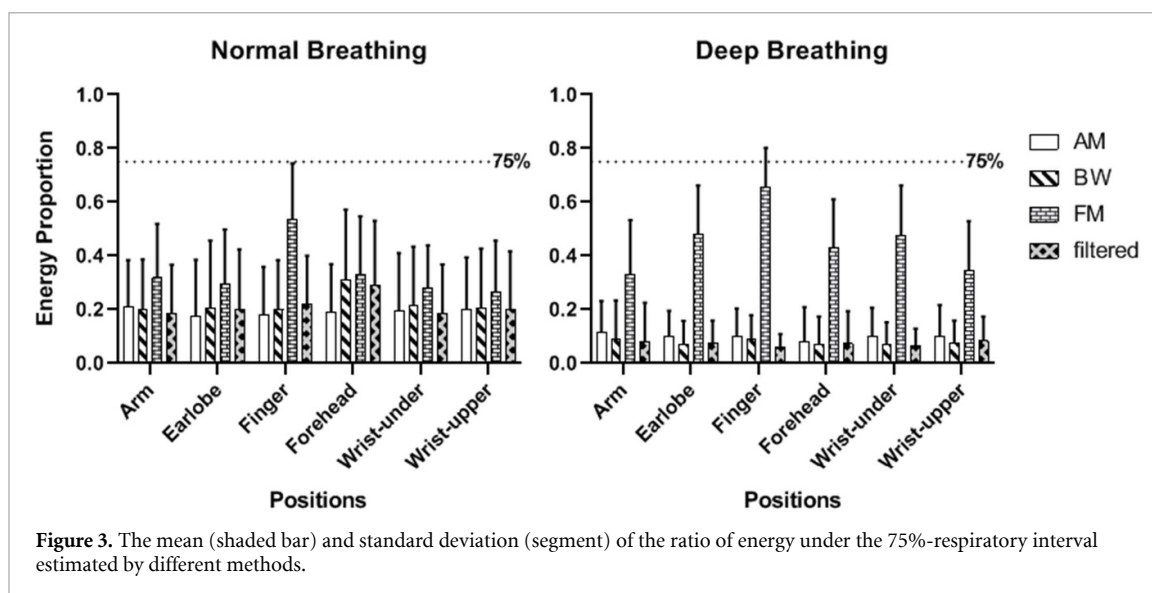


Table 1. The results of Dunn's Kruskal–Wallis multiple comparisons of RF derived by different methods in normal breathing. Significant difference is marked by *.

Data pair	Adjusted significance
Resp–AM	<0.001*
Resp–BW	<0.001*
Resp–FM	0.102
Resp–filtered	<0.001*
AM–BW	0.498
AM–FM	<0.001*
AM–filtered	0.889
BW–FM	<0.001*
BW–filtered	0.462
FM–filtered	<0.001*

Significant difference is marked by *.

3.2. RF values: respiratory frequency derived from PPG and a respiratory belt at different sites

The results showed that FM derived the most accurate RF estimation, particularly for normal breathing where FM was the only method for which the RF estimation was not significantly different from the reference value ($p > 0.05$).

Normal breathing: In normal breathing, the assumption of homogeneity of variance was violated in RF distribution ($p < 0.01$ in Levene's test). The results of the Scheirer–Ray–Hare test showed that there was a significant influence of extraction method ($p < 0.01$) on RF. FM achieved the most accurate RF estimation. The influences of measurement site or the interaction between measurement site and extraction method were not significant ($p > 0.05$ for both).

Dunn's Kruskal–Wallis multiple comparisons showed that there was no significant difference between the reference RF and the RF derived by FM, whereas RFs derived by AM, BW and filtering were significantly different from reference RF but were not significantly different from each other (table 1). No significant difference was observed between any two different measurement sites.

Deep breathing: In deep breathing, the assumption of homogeneity of variance was violated in RF distribution ($p < 0.01$ in Levene's test). The results of the Scheirer–Ray–Hare test showed that both extraction method and measurement site had a significant influence on RF ($p < 0.01$ for both). The influence of the interaction between measurement site and extraction method was not significant ($p > 0.05$).

Dunn's Kruskal–Wallis multiple comparisons showed that there was no significant difference between the reference RF and PPG-derived RFs derived by BW, FW or filtering (table 2). However, the RF derived by AM was significantly different from the reference RF and the RFs derived by FM and filtering. As to measurement sites, a significant difference was observed between finger and forehead, and between finger and wrist-upper ($p < 0.05$ for both).

Table 2. The results of Dunn's Kruskal–Wallis multiple comparisons of RF derived by different methods for deep breathing.

Data pair	Adjusted significance
Resp–AM	0.010*
Resp–BW	0.262
Resp–FM	0.268
Resp–filtered	0.917
AM–BW	0.134
AM–FM	<0.001*
AM–filtered	0.009*
BW–FM	0.025*
BW–filtered	0.278
FM–filtered	0.259

Significant difference is marked by *.

Table 3. The results of Dunn's Kruskal–Wallis multiple comparisons of ERF derived by different methods in normal breathing.

Data pair	Adjusted significance
AM–BW	0.709
AM–FM	<0.001*
AM–filtered	0.238
BW–FM	<0.001*
BW–filtered	0.361
FM–filtered	<0.001*

Significant difference is marked by *.

Table 4. The results of Dunn's Kruskal–Wallis multiple comparisons of ERF derived by different methods in deep breathing.

Data pair	Adjusted significance
AM–BW	0.090
AM–FM	<0.001*
AM–filtered	0.021*
BW–FM	0.025*
BW–filtered	0.411
FM–filtered	0.112

Significant difference is marked by *.

3.3. ERF values: the estimation error of PPG-based methods

Overall, FM showed the least estimation error. The ERF of FM was significantly smaller than those of AM, BW and filtering in both normal breathing ($p < 0.05$ for all), and than those of AM and BW in deep breathing ($p < 0.05$ for both).

Normal breathing: In normal breathing, the assumption of homogeneity of variance was violated in RF distribution ($p < 0.01$ in Levene's test). The results of the Scheirer–Ray–Hare test showed that there was a significant influence of extraction method ($p < 0.01$) on RF. FM achieved the least ERF. The influences of measurement site or the interaction between measurement site and extraction method were not significant ($p > 0.05$ for both).

Dunn's Kruskal–Wallis multiple comparisons showed that there was no significant difference between ERFs derived by AM, BW and filtering ($p > 0.05$ for all). The ERF derived by FM was significantly different from those derived by AM, BW and filtering ($p < 0.01$ for all), as shown in table 3.

Deep breathing: In deep breathing, the assumption of homogeneity of variance was violated in RF distribution ($p < 0.01$ in Levene's test). The results of the Scheirer–Ray–Hare test showed that the influences of extraction method and measurement site on RF were significant ($p < 0.01$ for both). The influence of the interaction between measurement site and extraction method was not significant ($p > 0.05$).

Dunn's Kruskal–Wallis multiple comparisons showed that significant differences in ERF existed between AM and FM, between AM and filtering, and between BW and FM (table 4). There was a significant difference between finger and wrist-upper on ERF ($p = 0.004$). The difference between finger and forehead was at the threshold of significance ($p = 0.053$) and the difference between finger and wrist-under just outside the threshold ($p = 0.057$). There was no significant difference in ERF between other measurement sites ($p > 0.05$ for all).

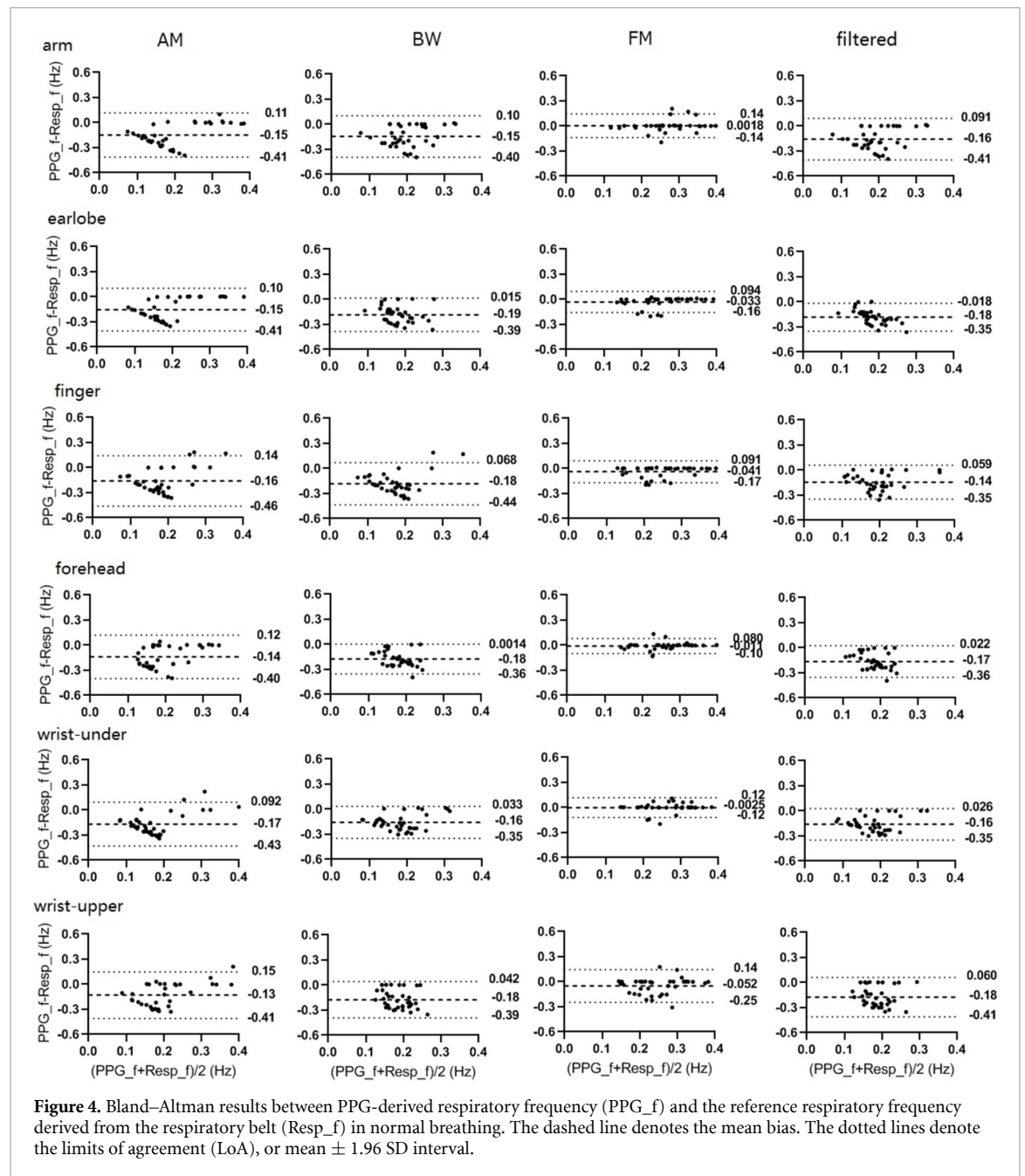


Figure 4. Bland–Altman results between PPG-derived respiratory frequency (PPG_f) and the reference respiratory frequency derived from the respiratory belt (Resp_f) in normal breathing. The dashed line denotes the mean bias. The dotted lines denote the limits of agreement (LoA), or mean \pm 1.96 SD interval.

3.4. Bland–Altman analysis

Normal breathing: In figure 4, the RFs derived by FM have the lowest bias and the narrowest limits of agreement (LoA) in all the sites and extraction methods. In the results of Bland–Altman analysis, all the values were rounded to the second significant digit to ensure that the small values (absolute value < 0.001 Hz, figure 5) could be accurately delineated. Therefore, the FM results were slightly different from those in our previous work where the data were rounded to two decimal places before Bland–Altman analysis (Hartmann et al 2019). The results are in accordance with the analysis of RF and ERF values. Therefore, FM was significantly more accurate than other methods in RF estimation. The other three methods (AM, BW and filtering) were comparable and less accurate in RF estimation. Especially, AM had the widest LoA in all the sites.

Deep breathing: In figure 5, the difference between different extraction methods depends on the site. All the methods achieved small biases (< 0.025 Hz) in all the measurement sites, which is equal to less than 1.5 breaths per minute. The highest biases (-0.021 Hz and -0.024 Hz) were derived by AM. The LoA of AM was always the widest except in finger. This is in accordance with the RF and ERF results that only the AM-derived RF value was significantly different from the reference RF. The other three methods did not show a consistent difference in accuracy in all the sites.

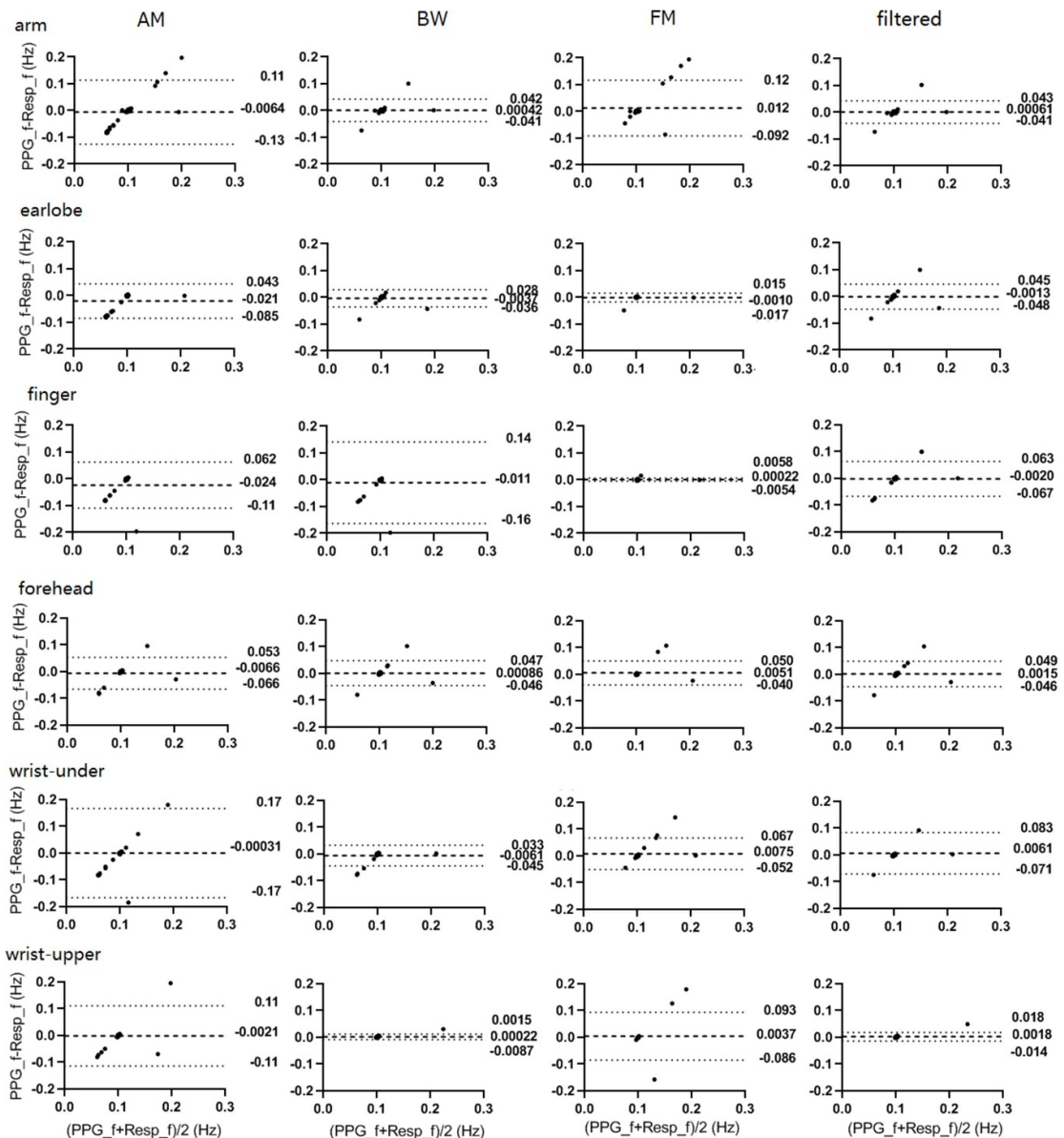


Figure 5. Bland–Altman results between PPG-derived respiratory frequency (PPG_f) and the reference respiratory frequency derived from the respiratory belt (Resp_f) in deep breathing. The dashed line denotes the mean bias. The dotted lines denote the limits of agreement (LoA), or mean \pm 1.96 SD interval.

4. Discussion

In this study, based on the analysis of related physiological mechanisms, the strength of four respiratory modulations, as well as the accuracy of RF estimation, were compared in different measurement sites, and normal and deep breathing patterns, respectively. It is an important supplement to our existing study (Hartmann *et al* 2019), and provides a reference for related studies. On the one hand, the results of our study can provide a reference for physiological studies on the modelling of PPG signal (Khoo and Chalacheva 2019) and the estimation of respiratory effect on peripheral hemodynamic oscillations (Tankanag *et al* 2020). On the other hand, our results shed light on the fusion of different respiratory-induced modulations. Currently, in the fusion of respiratory signals or RF estimations derived from different respiratory modulations of PPG signals, the calculation of the weights mainly depends on the analysis of the respiratory signals, with a lack of consideration of different physiological conditions (Liu *et al* 2019, Pollreisz and Nejad 2020, Pirhonen and Vehkaoja 2020). According to our results, the weights should be adjusted in different breathing patterns and different measurement sites (e.g. BW achieved the most accurate estimation of RF at the wrist-upper and wrist-under sites in deep breathing) to achieve more accurate estimation of RF.

4.1. Different respiratory modulations in both breathing patterns

In normal breathing, FM was the only method whose derived RF was not significantly different from the reference RF. The estimation error was significantly less than the other three methods. In Bland–Altman analysis, FM had the lowest bias and the narrowest LoA in all the sites. The energy proportion of FM was also significantly higher than the values from the other methods. Therefore, in normal breathing, the modulation by FM had the highest strength of respiratory modulation and the highest accuracy in RF estimation.

In deep breathing, the estimations of RF derived by BW, filtering and FM were not significantly different from the reference RF. However, the ERF of FM was significantly different from the corresponding results of AM and BW. In Bland–Altman analysis, the lowest bias and narrowest LoA belonged to BW and FM in different sites. The energy proportion of FM was significantly higher than all the other methods. Therefore, in deep breathing, FM still had the highest strength of respiratory modulation, but its accuracy in RF estimation was comparable with BW and filtering.

Compared with normal breathing, in deep breathing the energy proportion was higher in FM but lower in other methods. In deep breathing, many different mechanisms of blood flow regulation are activated, resulting in cardiorespiratory vagal afferents, the oscillations in cerebral blood flow, enhanced Mayer–Traube–Hering waves, and finally the interference on AM and BW, resulting in a lower energy proportion (Noble and Hochman 2019). In deep breathing, with the involvement of neural sympathetic activity, the respiration–vasomotion coupling is intensified (Ovadia-Blechman *et al* 2017), which will lead to the variation of impedance in peripheral microcirculation. The enhanced neural activity might be related to the lower energy proportion in deep breathing. Deep breathing could decrease the amplitude of BP and its cardiac fluctuations (Dick *et al* 2014) but increase its respiratory fluctuations (Nuckowska *et al* 2019). Therefore, despite the lower respiratory energy proportion, the error in RF estimation was lower in deep breathing for AW, BW and filtering (figures 4 and 5). The RSA which causes RF is greatly exaggerated at slower respiratory frequencies as the difference between the maximal and minimal heart rates is enlarged (Noble and Hochman 2019).

The difference in respiratory modulations is related to physiological mechanisms. As shown in figure 1, AM and BW were related to many different mechanisms. In particular, the baroreflex is the major mechanism that maintains the beat-to-beat blood pressure (Kishi 2018) which may activate other mechanisms of hemodynamic regulation. Li *et al* compared the intensities of FM, AM and BW in PPG signals using the correlation coefficients with reference respiratory signal (Li *et al* 2010). They found that the strength of FM was higher than AM and BW, which is consistent with the results of our analysis of energy proportion. However, Li *et al* did not perform any statistical analysis. The authors compared the difference between sitting and lying postures, and between males and females. A study suggested that age and gender have insignificant effects ($p = 0.67$) on the respiratory modulation of PPG signals (Nilsson *et al* 2006). Therefore, in this pilot study, we just focused on the strength of different respiratory modulations on PPG signal and considered the effect of measurement site which significantly influences the PPG waveform (Hartmann *et al* 2019).

4.2. Accuracy of RF estimation by different demodulations

In this study, the FM method showed the highest accuracy in RF estimation compared with other methods. For PPG signals, the method of demodulation could influence the accuracy of derived respiratory signal and RF estimation. Yang *et al* (2019) compared AM, BW, and FM in the accuracy of RR estimation. As found in our study, they concluded that FM was more accurate than BW and AM and in a normal range of RR ($12\text{--}15\text{ breaths min}^{-1}$), and BW is better than AM. However, they used the interval of systolic peaks to derive FM. In the PPG signal, the position of the systolic peak point is sensitive to noises and filtering. Karlen *et al* investigated three respiratory-induced variations (frequency, intensity and amplitude, corresponding to FM, BW and AM respectively), whose errors are 5.8, 6.2, and 3.9 breaths min^{-1} (0.097, 0.103, and 0.065 Hz) in estimating RR from PPG signal (Karlen *et al* 2013). They used peak values and intervals between peaks to calculate the variations of intensity and frequency, which affected the accuracy of AM and FM, respectively. In detecting FM of PPG signal, the maximum slope point has been proven to be more reliable for measuring RF than peak or valley point which is prone to non-trivial error due to common artifacts in the waveforms and wave reflection interference (Escobar and Torres 2014). Firstly, as to the PPG signal in a cardiac cycle, the slope of systolic uprising side is much higher than the value of any other segment. It is difficult for the motion artefacts or other noises superimposed to the PPG signal to affect the waveform severely and move the maximum slope point out of the systolic uprising side. Secondly, the time length of systolic uprising side is short ($<0.15\text{ s}$). The change in the intensity of motion artefact or other noises is limited in such a short period, which makes the position of maximum slope point reliable. Finally, considering the obvious change in the cardiac cycle length caused by respiration, even the position of maximum slope point is inaccurate, as long as it is in the systolic uprising side, the effect on FM detection is limited. Therefore, the FM detection based on maximum slope point is reliable and robust to the noises. In comparison, the accurate detection of

peak and valley points is difficult, which limited the accuracy of AM and BW in estimating RF. Due to its smoothly shaped peaks, finding fiducial points (including peaks and valleys) in PPG is more challenging than in electrocardiography (Firoozabadi *et al* 2017). It has been known that fiducial features of PPG signals are sensitive to noises including motion artefacts (Karimian *et al* 2017). Additionally, the detection of fiducial points can be influenced by the filtering. The visual inspection of PPG waveforms showed that the shape distortion was particularly obvious at the pulse peaks when a high pass filter was applied with the cut-off frequency higher than 0.2 Hz (Allen and Murray 2004). There is a need for an advanced signal processing method to improve the reliability and robustness of RF estimation based on AM and BW methods.

4.3. Factors influencing the accuracy of demodulation-based RF extraction

The difference between measurement sites is inconsistent in normal and deep breathing patterns, and in RF, ERF and energy proportion. In figure 3, finger has the highest energy proportion which means its position of RF in the frequency domain has the highest accordance with the reference RF. In figure 1, the PPG signal depends on the impedance of arteries, as well as sensor attachment. The impedance of peripheral arteries that supply the blood flow to the finger is less affected by the respiration compared with other proximal arteries. It has been shown that the PPG signal from finger has the lowest ratio between cardiac and respiratory pulse energies (Nilsson *et al* 2007), compared with wrist, arm and forehead. In figure 6(a), the amplitudes of PPG-derived respiratory signals are much lower than the amplitude of PPG fluctuation in a cardiac cycle. The finger is also the best place to get a reliable attachment. Therefore, although finger has a low strength of respiratory modulations, its PPG waveform shows the minimal influence of neural regulations as compared with the forehead PPG waveform. A recent study suggested that PPG signal from finger is more accurate in RF estimation compared with forehead and wrist (Longmore *et al* 2019). In contrast, the PPG signal from the forehead has been known to be affected by lower frequency (0.1 Hz–0.2 Hz) baseline fluctuations of PPG signals, which are evident in humans as part of a separate vascular response to the sympathetic nervous system. These fluctuations are often referred to as Mayer–Traube–Hering waves and are thought to represent the baroreflex mediated oscillation of arterial blood pressure (Meredith *et al* 2012). This component could significantly influence the PPG signal of forehead and cause inaccuracy in RF estimation (Hernando *et al* 2019). In figure 6(a), the PPG waveform of forehead has large fluctuations in baseline. As a result, the frequency peaks derived by AM, BW and filtering are located between 0 Hz–0.15 Hz.

4.4. Limitations and future directions

In this pilot study, firstly, the number of subjects is limited. Especially, a major limitation is that only young and healthy individuals are included. It is interesting that the results presented in this study are in agreement with the results for young healthy adults (aged 18–39) in Charlton *et al*'s work where the FM modulation was the strongest in young healthy subjects, but much weaker in elderly healthy subjects (Charlton *et al* 2017b). It is well known that heart rate variability and RSA decreases with age (Charlton *et al* 2017b). It has been found that RSA in the older subjects (59 to 71 years) was <20% of that in the younger subjects (20 to 31 years) (Kaushal and Taylor 2002). Therefore, the conclusion from this study cannot be generalized to other populations. More subjects are needed to further investigate the effect of age, gender and race on respiratory modulations of PPG signal. Secondly, all the data were recorded in sitting posture. The blood flow in microcirculation will change in different postures. Moreover, a recent study shows that posture may influence the respiratory FM in PPG signal (Sahroni *et al* 2019). Additionally, during measurement, the subjects were given enough resting time and were asked to breath as stably as possible. However, it was difficult for each subject to reach an ideally steady breathing state. The calculated RF was an estimation of the averaged RF during the period of measurement instead of the real-time value. Finally, as a pilot study, the analysis of physiological mechanisms of respiratory modulations is not conclusive. In future studies, more subjects in different postures and physiological conditions (e.g. post-exercise measurements) could be included for a more comprehensive evaluation of respiratory modulations of PPG signals. More advanced algorithms are needed to achieve real-time monitoring of RF.

5. Conclusion

Of all the respiratory modulations, FM has the highest strength and is appropriate for accurate RF estimated based on PPG signal recorded in different sites and breathing patterns. Compared with other positions, the finger showed the strongest FM. The physiology of different respiratory modulations of PPG signals deserves further investigation and will provide a reference for the algorithms of RF extraction from PPG signals.

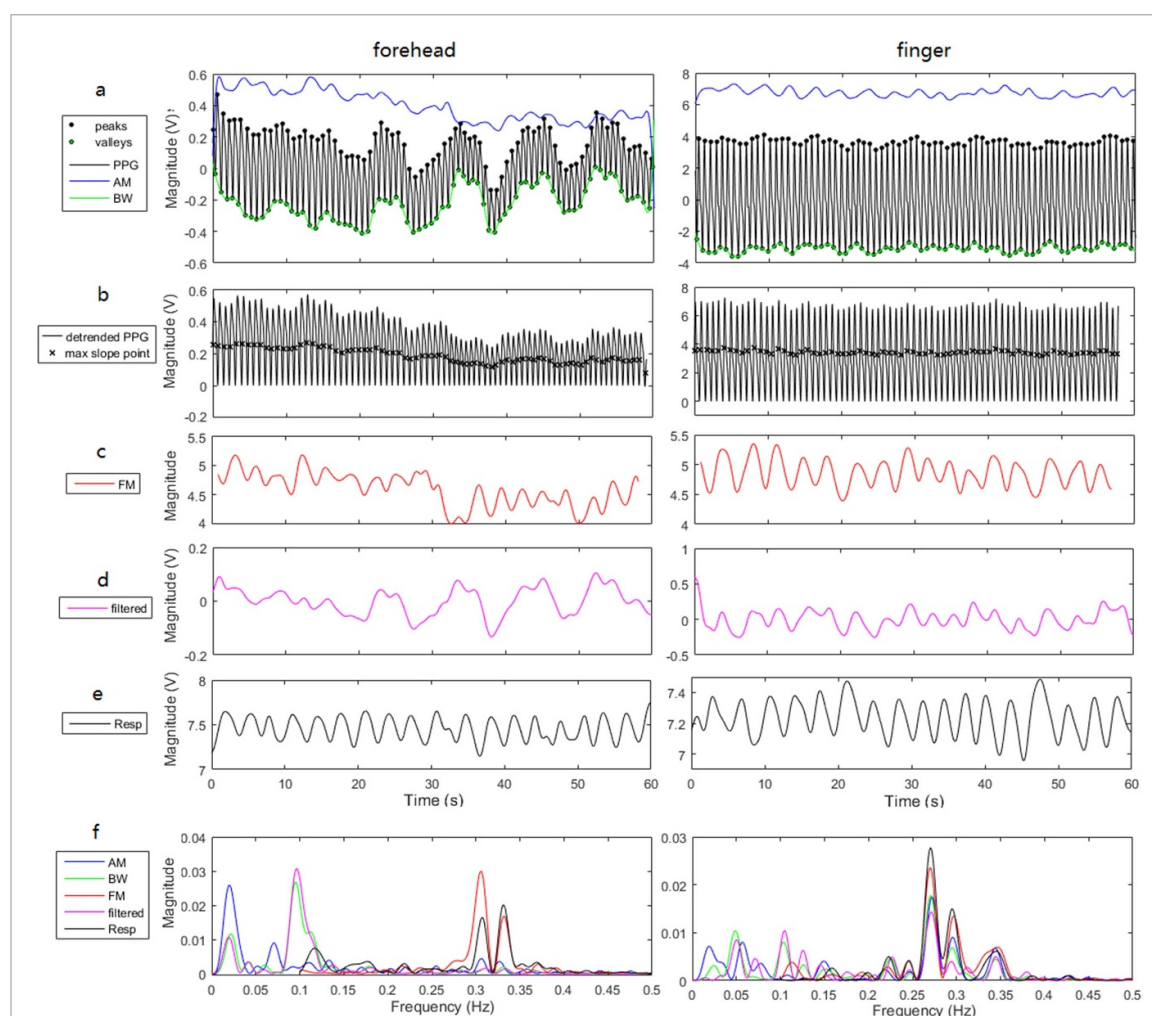


Figure 6. RF estimations in forehead and finger of the same subject. (a) Extraction of peaks and valleys from filtered PPG signal. The blue and green lines denote the derived respiratory signals by AM and BW. (b) Extraction of maximal slope points (the crosses) from detrended PPG signal. (c) Respiratory signal derived by FM. (d) Respiratory signal derived by filtering. (e) Reference respiratory signal (Resp) recorded by strain gauge. (f) Extraction of RF from different respiratory signals using PSD.

Acknowledgments

This study is supported by the National Natural Science Foundation of China (Grant No. 61828104), the Basic Research Foundation of Shenzhen (Grant No. JCYJ20160509162237418), and the Newton Funds Industry Academia Partnership Programme (Grant No. IAPP1R2/100204). We acknowledge Wentao Hong and Mingtao Li for their suggestions and assistance in the programming with Matlab. We acknowledge Aleksandra Wingert for reviewing the paper and correcting the grammatical errors.

ORCID iDs

Haipeng Liu  <https://orcid.org/0000-0002-4212-2503>

Fei Chen  <https://orcid.org/0000-0002-6988-492X>

References

- Allen J and Murray A 2004 Effects of filtering on multisite photoplethysmography pulse waveform characteristics *Computers in Cardiology 2004* (IEEE) pp 485–8
- Birrenkott D A, Pimentel M A, Watkinson P J and Clifton D A 2018 A robust fusion model for estimating respiratory rate from photoplethysmography and electrocardiography *IEEE Trans. Biomed. Eng.* **65** 2033–41
- Charlton P H, Birrenkott D A, Bonnici T, Pimentel M A, Johnson A E, Alastruey J, Tarassenko L, Watkinson P J, Beale R and Clifton D A 2017a Breathing rate estimation from the electrocardiogram and photoplethysmogram: A review *IEEE Rev. Biomed. Eng.* **11** 2–20
- Charlton P H, Bonnici T, Tarassenko L, Alastruey J, Clifton D A, Beale R and Watkinson P J 2017b Extraction of respiratory signals from the electrocardiogram and photoplethysmogram: technical and physiological determinants *Physiol. Meas.* **38** 669–90
- Dick T E, Mims J R, Hsieh Y-H, Morris K F and Wehrwein E A 2014 Increased cardio-respiratory coupling evoked by slow deep breathing can persist in normal humans *Respir. Physiol. Neurobiol.* **204** 99–111

- Escobar B and Torres R 2014 Feasibility of non-invasive blood pressure estimation based on pulse arrival time: a MIMIC database study *Computing in Cardiology 2014* pp 1113–6
- Firoozabadi R, Helfenbein E D and Babaeizadeh S 2017 Efficient noise-tolerant estimation of heart rate variability using single-channel photoplethysmography *J. Electrocardiol.* **50** 841–6
- Hartmann V, Liu H, Chen F, Hong W, Hughes S and Zheng D 2019 Towards accurate extraction of respiratory frequency from the photoplethysmogram: effect of measurement site *Frontiers Physiol.* **10** 732
- Hernando A, Peláez-Coca M D, Lozano M T, Lázaro J and Gil E 2019 Finger and forehead PPG signal comparison for respiratory rate estimation *Physiol. Meas.* **40** 095007
- Johansson A 2003 Neural network for photoplethysmographic respiratory rate monitoring *Med. Biol. Eng. Comput.* **41** 242–8
- Karimian N, Guo Z, Tehranipoor M and Forte D 2017 Human recognition from photoplethysmography (PPG) based on non-fiducial features 2017 *IEEE Int. Conf. Acoustics, Speech and Signal Processing (ICASSP)* (IEEE) pp 4636–40
- Karlen W, Raman S, Ansermino J M and Dumont G A 2013 Multiparameter respiratory rate estimation from the photoplethysmogram *IEEE Trans. Biomed. Eng.* **60** 1946–53
- Kaushal P and Taylor J A 2002 Inter-relations among declines in arterial distensibility, baroreflex function and respiratory sinus arrhythmia *J. Am. Coll. Cardiol.* **39** 1524
- Khoo M C K and Chalacheva P 2019 Respiratory modulation of peripheral vasoconstriction: a modeling perspective *J. Appl. Physiol.* **127** 1177–86
- Kiselev A R, Karavaev A S, Gridnev V I, Prokhorov M D, Ponomarenko V I, Borovkova E I, Shvartz V A, Ishbulatov Y M, Posnenkova O M and Bezruchko B P 2016 Method of estimation of synchronization strength between low-frequency oscillations in heart rate variability and photoplethysmographic waveform variability *Russ. Open Med. J.* **5** 0101-
- Kishi T 2018 Baroreflex failure and beat-to-beat blood pressure variation *Hypertension Res.* **41** 547–52
- Li J, Jin J, Chen X, Sun W and Guo P 2010 Comparison of respiratory-induced variations in photoplethysmographic signals *Physiol. Meas.* **31** 415–25
- Liu H, Allen J, Zheng D and Chen F 2019 Recent development of respiratory rate measurement technologies *Physiol. Meas.* **40** 07TR1
- Longmore S K, Lui G Y, Naik G, Breen P P, Jalaludin B and Gargiulo G D 2019 A comparison of reflective photoplethysmography for detection of heart rate, blood oxygen saturation, and respiration rate at various anatomical locations *Sensors* **19** 1874
- Meredith D J, Clifton D, Charlton P, Brooks J, Pugh C W and Tarassenko L 2012 Photoplethysmographic derivation of respiratory rate: a review of relevant physiology *J. Med. Eng. Technol.* **36** 1–7
- Nilsson L, Goscinski T, Johansson A, Lindberg L-G and Kalman S 2006 Age and gender do not influence the ability to detect respiration by photoplethysmography *J. Clin. Monit. Comput.* **20** 431–6
- Nilsson L, Goscinski T, Kalman S, Lindberg L G and Johansson A 2007 Combined photoplethysmographic monitoring of respiration rate and pulse: a comparison between different measurement sites in spontaneously breathing subjects *Acta Anaesthesiol. Scand.* **51** 1250–7
- Nilsson L, Johansson A and Kalman S 2000 Monitoring of respiratory rate in postoperative care using a new photoplethysmographic technique *J. Clin. Monit. Comput.* **16** 309–15
- Noble D J and Hochman S 2019 Hypothesis: pulmonary afferent activity patterns during slow, deep breathing contribute to the neural induction of physiological relaxation *Frontiers Physiol.* **10** 1176
- Nuckowska M K, Gruszecki M, Kot J, Wolf J, Guminski W, Frydrychowski A F, Wtorek J, Narkiewicz K and Winkowski P J 2019 Impact of slow breathing on the blood pressure and subarachnoid space width oscillations in humans *Sci. Rep.* **9** 6232
- Orphanidou C 2017 Derivation of respiration rate from ambulatory ECG and PPG using ensemble empirical mode decomposition: comparison and fusion *Comput. Biol. Med.* **81** 45–54
- Ovadia-Blechman Z, Gavish B, Levy-Aharoni D, Shashar D and Aharonson V 2017 The coupling between peripheral microcirculation and slow breathing *Med. Eng. Phys.* **39** 49–56
- Pirhonen M and Vehkaoja A 2020 Fusion enhancement for tracking of respiratory rate through intrinsic mode functions in photoplethysmography *Biomed. Signal Process. Control* **59** 101887
- Pollreis D and Nejad N T 2020 Reliable respiratory rate extraction using PPG 2020 *IEEE 11th Latin American Symp. on Circuits & Systems (LASCAS)* (IEEE) pp 1–4
- R Core Team 2019 'R: A language and environment for statistical computing' R Foundation for Statistical Computing V, Austria www.R-project.org/
- Sahroni A, Hassya I A, Rifaldi R, Jannah N U, Irawan A F and Rahayu A W 2019 HRV assessment using finger-tip photoplethysmography (PulseRate) as compared to ECG on healthy subjects during different postures and fixed breathing pattern *Procedia Comput. Sci.* **161** 535–43
- Sailer A M, Wagemans B A J M, Das M, de Haan M W, Nelemans P J, Wildberger J E and Schurink G W H 2015 Quantification of respiratory movement of the aorta and side branches *J. Endovascular Ther.* **22** 905–11
- Tankanag A V, Grinevich A A, Tikhonova I V and Chemeris N K 2020 An analysis of phase relationships between oscillatory processes in the human cardiovascular system *Biophysics* **65** 159–64
- Yang H, Li M, He D, Che X and Qin X 2019 Respiratory rate estimation from the photoplethysmogram combining multiple respiratory-induced variations based on SQI 2019 *IEEE Int. Conf. Mechatronics and Automation (ICMA)* (IEEE) pp 382–7